Journal of Alloys and Compounds 501 (2010) 70–76

Contents lists available at ScienceDirect

Journal of Alloys and Compounds

journal homepage: www.elsevier.com/locate/jallcom

On phase transition velocities of NiTi shape memory alloys

W.G. Guo [a,*], J. Su [a], Y. Su [b], S.Y. Chu [a]

[a] School of Aeronautics, Northwestern Polytechnical University, No. 127, Youyi West Rd., Xi'an 710072, PR China
[b] School of Aerospace Engineering, Beijing Institute of Technology, Beijing 100081, PR China

ARTICLE INFO

Article history:
Received 12 January 2010
Received in revised form 22 March 2010
Accepted 1 April 2010
Available online 10 April 2010

Keywords:
NiTi SMAs
Martensite
Phase transformation
Strain rate
Temperature

ABSTRACT

Two important velocities of austenite–martensite phase transformation in NiTi shape memory alloys (SMAs) have been experimentally investigated in this work: the velocity of stress-induced martensitic transformation upon mechanical loading and the recovery velocity for thermally driven and mechanically detwinned martensitic phase to transform back to austenite upon heating. To measure the velocity for stress-induced martensitic transition, a series of uniaxial compressive loading tests have been performed for both quasi-static and dynamic loading conditions, using an Instron servohydraulic testing machine and enhanced Hopkinson bar facilities, respectively. A pulse shaper has been employed during the Hopkinson bar dynamic loading test to obtain constant loading and unloading strain rates. According to the testing results, the velocity limit for a stress-induced martensitic transition in samples NiTi-A can be measured as the highest observed deforming velocity that allows pseudoelastic behaviors. It is also found that martensitic transformation stress, σ_{tr}, tends to approach to a constant value when strain rate is above 0.1/s. To understand the thermally driven recovery velocity for reverse martensitic transformation, however, samples of NiTi-B, in martensitic twins, are firstly detwinned by uniaxial loading at room temperature, and then heated to recover their austenite phase. Multi-point temperature increase tests and fixed temperature tests are performed. It is observed that the recovery velocity is approaching to an upper bound of 0.014 mm/s. A few other noteworthy observations have been obtained as well.

1. Introduction

It is well known that NiTi shape memory alloys (SMAs) may experience temperature-induced or stress-induced phase transformation upon temperature change or external loading. These two types of phase transformation are believed to cause the so called "shape memory effect" and "pseudoelasticity" (sometimes "superelasticity"), respectively. After being thermally driven to martensitic phase, NiTi SMAs can sustain large deformation due to the reorientation of martensitic twins, and the shape memory effect occurs when the material is then heated to a temperature above the austenite finish temperature, A_f, to complete the reverse transformation. Since there is only one possible orientation for the parent phase (austenite), all martensitic configurations revert to the original crystal structure and the original shape is restored. This effect causes the deformed specimen to recover completely, and thus, the material "remembers" its original shape. The other important characteristic, pseudoelasticity, refers to the ability of NiTi SMAs to return to its original shape upon unloading after substantial deformation while the temperature always stays above A_f. By observing the crystal lattice structures of NiTi SMAs, one notices that the austenitic phase has a cubic lattice (B2) while the martensitic phase is with monoclinic lattice (B19) [1], consisting of only lattice twins. In the past decade, the thermomechanical response and pseudoelastic behavior of NiTi SMAs under different conditions have been extensively studied [1–6]. Now the shape memory effect and pseudoelasticity of NiTi SMAs have been widely adopted in many fields. For instance, solid-state sensors and actuators with SMAs springs have been used for detection and localization of fire in many suppression and extinguishing systems [7]; SMAs play an increasing role in a broad range of applications in micro-electromechanical systems (MEMS) (also referred to as microsystems), such as automotive parts, consumer products or biomedical devices [8,9]; with the help of stop structures, SMAs springs on a morphing aerofoil can accurately drive certain control points on the aerofoil skins to achieve the target profile [10]; and SMAs can also be used in shock-absorbing devices with the aid of stop structures. In all of these above-mentioned applications, the velocities for phase transition between austenite and martensite in NiTi SMAs are key factors to evaluate the devices' efficiency, applicability and reliability. Tobushi et al. [11] carried out dynamic tensile loading tests and found that, for a

* Corresponding author. Tel.: +86 29 88493386; fax: +86 29 88494859.
E-mail address: weiguo@nwpu.edu.cn (W.G. Guo).

0925-8388/$ – see front matter © 2010 Elsevier B.V. All rights reserved.
doi:10.1016/j.jallcom.2010.04.031

strain rate higher than 0.1/min, the martensitic transformation stress and measured temperature will increase with an increasing strain rate during the loading process; but the critical transition stress and measured temperature for reverse transformation will decrease as the unloading strain rate gets lower. Liu et al. [12] pointed out that when the strain rate changes from 3×10^{-4} to 3000/s, the characteristics of the stress–strain curve also change accordingly, which implies the sensitivity to the strain rate. They also showed that the stabilization of the detwinned martensitic phase after deformation appears to be independent to the strain rate.

These published results indicated that the applied strain rate has a significant effect on the stress-induced phase transition, and consequently changes the constitutive behavior. On the other hand, one may expect that the ability and velocity of phase transition might also be determined by analyzing the stress–strain behaviors at different strain rates during the tests. For instance, one can investigate the velocity for stress-induced martensitic phase transition by finding out the limit of maximum applied strain rate that can keep the transformation going. This is because, for any applied strain rate higher than that, the deforming velocity is beyond the ability and intrinsic velocity of martensitic transition such that the overall constitutive behavior is dominated by deforming mechanisms other than phase transition. Therefore in Section 2, we provide related theories to martensitic phase transition, theoretical estimate of the intrinsic transition velocity, and a proposed approach for experimental investigation. In Sections 3.1 and 3.2, we describe the preparation of specimens and discuss the temperature caused by stress-induced martensitic transformation; in Section 3.3, we are going to describe the method to obtain the velocity for stress-induced martensitic phase transformation through pseudoelastic loading tests; in Section 3.4 we discuss the tests to measure the recovery velocity for the thermally driven and mechanically detwinned martensitic phase to transform back to austenite by heating. That means the material is subject to no mechanical loading and is heated to initiate the shape memory effect. A few noteworthy conclusions are finally obtained in Section 4.

2. Theory and basic assumptions

2.1. Fundamentals to the austenite–martensite transformation

As depicted in Fig. 1, NiTi SMAs are able to have diffusionless martensitic transformation, either upon cooling or applied stress. It makes SMAs exhibit two distinct responses accordingly. Usually detwinning, i.e., an energetically favored martensite variant growing at the expense of the others, occurs when SMAs are deformed below the martensite finish temperature, M_f. After being heated, SMAs can recover their original shape due to the reverse transformation, which is corresponding to the shape memory effect. Pseudoelasticity (or sometimes called superelasticity) appears due to the stress-induced martensitic transformation when the SMAs are being deformed in the austenitic state at a temperature above A_f. The original shape of SMAs can usually be completely recovered by releasing the applied load. For instance, Fig. 2 shows a typical pseudoelastic stress–strain behavior of NiTi SMA upon quasi-static compressive loading and unloading. The point of the first slope change corresponds to the initiation of martensitic transformation. The phase transition keeps going upon loading until the slope remains constant again, which means the martensitic transition has completed. The martensitic phase will transform back to austenite upon unloading and the strain can be completely recovered. Therefore the whole microscopic phase transition process can be captured by the characteristics of pseudoelasticity. In another words, the initiation, course, and completeness of stress-induced martensitic transformation can all be recognized in the stress–strain curves.

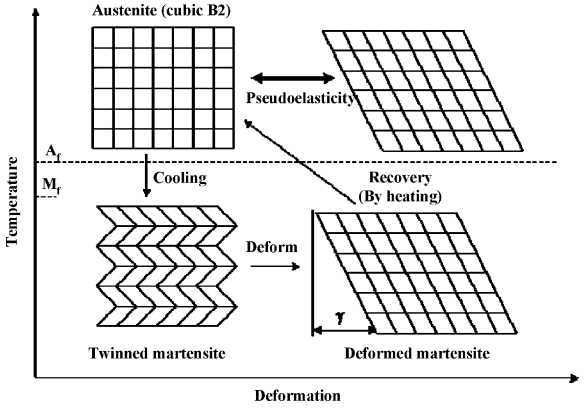

Fig. 1. Schematic illustration of lattice structure changes between the austenite (B2) and the martensite phase (B19).

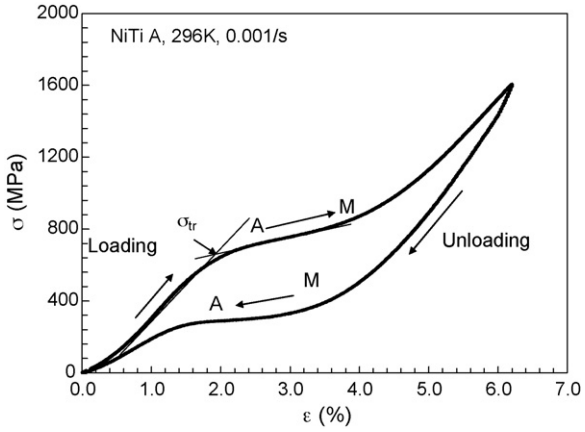

Fig. 2. Pseudoelastic behavior of NiTi-A at a strain rate of 10^{-3}/s.

Deformation or strain in NiTi SMAs is generally a result of phase transformation in a crystal structure point of view. Austenite is commonly referred to as the parent phase or high-temperature phase with cubic structure (B2) and martensite as the low-temperature phase usually with tetragonal (B19) crystal structure. The cubic structure (B2) can transform to tetragonal (B19) (twinned) upon cooling. During this procedure intermediate R phase can be nucleated in B2 phase. The phase transition is believed to be diffusionless shear transformation. Deformation of martensite causes detwinning and consequently moves twin boundaries. The detwinned tetragonal structure will transform back to cubic austenite phase upon heating.

2.2. Theoretical estimate of the limit for the velocity of phase transformation

Now the question spontaneously arises to what extent can the velocity of phase transformation be? As a matter of fact a diffusionless martensitic transformation is required for the crystal lattice structure to accommodate to the minimum energy state for given temperature and loading conditions. Based on atomic vibration knowledge, see Fig. 3, the period of atomic vibration, T, is about 10^{-13} s. Depending on atomic lattice constant, the atomic disturbance distance, L, can be taken to be approximately $3\dot{A}$ or 3×10^{-10} m, where $\dot{A}$ is a metallic atomic radius [13]. Thus, the

motion velocity by atom itself may be written as

$$\omega = \frac{3\dot{A}}{T} = 3 \times 10^{-10} \times 10^{13} = 3 \times 10^{3} \text{ m/s}. \quad (1)$$

Eq. (1) provides a theoretical estimate of the velocity limit for phase transition with diffusionless atomic displacement of a crystal lattice structure. But it is known that atomic displacement suffers from various obstacles, which may cause a lower phase transition velocity than the theoretical limit. Therefore, in the following sections, a series of experimental studies are presented to evaluate the phase transition velocity of NiTi SMAs.

2.3. Proposed experimental approach to estimate the phase transition velocities

There are three basic assumptions in the proposed approach. (1) The procedure of austenite–martensite transition is not done instantaneously. Such transition takes place with an intrinsic velocity, and will need a responding time to complete. (2) Depending on the imposed strain rate, there exist two types of deformation mechanisms in SMAs: one is diffusionless phase transformation, where atoms move cooperatively on a shear-like mechanism. Such deformation mechanism leads to the pseudoelastic behavior, and the large strain will be recovered completely upon unloading. The other deformation mechanism is dislocation-based slip plasticity, and the residual deformation is permanent and will not recover upon unloading. (3) High imposed strain rate does not result in any major deformation mechanisms other than those described in (2).

With the theory of martensitic phase transition and the assumptions described above, we hereby propose an experimental approach to investigate the velocity of stress-induced martensitic transition. A series of uniaxial compressive loading and unloading tests are going to be performed with different imposed strain rates on NiTi SMAs. As we have assumed, the material has an intrinsic martensitic phase transition velocity. On one hand, if the phase transition process is faster than the imposed deformation, the austenitic phase eventually transforms to martensitic phase. The material shows a pseudoelastic constitutive behavior and sustains a large recoverable deformation. On the other hand, if the velocity of imposed deformation surpasses the martensitic transformation, the material does not have a chance to experience phase transformation, and slip plasticity deformation is driven to occur instead. The overall material will then show a linear constitutive relation with the stiffness of austenite followed by plastic deformation just like an ordinary homogenous solid under large imposed strain. Pseudoelasticity does not appear in such scenario and there will be residual strain upon the completeness of unloading. Starting from a relatively low strain rate, one keeps raising it during the compressive loading test. By the time the pseudoelastic behavior is completely gone, the corresponding velocity of imposed deformation should have reached the limit for stress-induce martensitic transformation. Based on the theory of austenite–martensite transformation in SMAs as described in Section 2.1, it is been widely believed that the observed constitutive behavior is actually a macroscopic reflection of the microstructural rearrangement [14]. Therefore the velocity of stress-induced martensitic transition can at least be qualitatively investigated through the method developed above.

Another phase transition velocity that can be experimentally investigated is the recovery velocity during the shape memory effect. One can study the effect of imposed temperature on the recovery velocity of thermally driven reverse martensitic transformation by direct measurement of the recovering strain rates and the corresponding applied temperatures. Detailed description of the corresponding tests for the phase transition velocities are given in the following section.

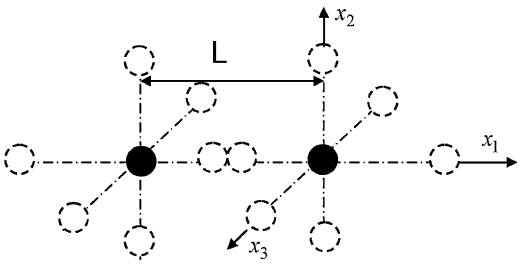

Fig. 3. Results from the compressive loading test for NiTi-A with a strain rate of 0.01/s at room temperature.

3. Experimental approaches and results

3.1. Testing materials and specimens

In this work, two types of SMA testing materials are used for separate purposes, and they are denoted as NiTi-A and NiTi-B, respectively. NiTi-A comes with 55.9Ni–44.1Ti (atom%) pseudoelastic wires with nominal diameter of 5 mm from Nitinol Devices and Components (NDC). NiTi-A's austenite finish temperature, A_f, is 263 K, and the material is in a stable austenitic state at room temperature of 296 K. NiTi-B comes with 50.8Ni–49.2Ti (atom%) plate strips with thickness of 2 mm provided by Chinese Northwestern SMA Inc. Its A_f is 333 K and the material is in a stable martensitic state at room temperature of 296 K. Samples of NiTi-A are machined into cylinders with nominal diameter of 4.5 mm and nominal length of 5 mm. Samples of NiTi-B are machined into dog-bone-shaped plates with an effective middle length of 35 mm.

3.2. Thermal measurement during the phase transformation

NiTi SMAs' property is strongly affected by temperature. It is also known that the phase transformation procedure will induce exothermic reactions. Therefore, one needs to understand the temperature rise induced by phase transition before doing the tests proposed in Section 2.3. To evaluate such temperature rise, several samples of NiTi-A are annealed at 773 K for 30 min, and then compressed at a strain rate of 0.01/s at room temperature, using an Instron servohydraulic testing machine. The samples and the compressive heads of the testing machine are heat-insulated with stone cotton material during testing process. A thermocouple with an accuracy of ±0.5 °C is directly attached to the samples to measure temperature changes. Three samples of NiTi-A are used for such test and very similar results have been obtained. The typical testing results are plotted in Fig. 4. In this plot, the curve, marked as "calculated", is corresponding to the temperature rise based on the following calculation:

$$\Delta T = \int_0^{\varepsilon} \frac{\beta}{\rho C_V} \sigma d\varepsilon, \quad (2)$$

where ρ is the constant for mass density of NiTi SMAs and C_V the temperature-dependent heat capacity. ε stands for the strain, σ the stress in MPa, and β the fraction of the total work done to be converted into heat. Here the mass density is taken to be 6.45 g/cc, heat capacity taken as 0.322 J/g K at room temperature, and the value of β is approximately 75%, while the other 25% is contributed to the elastic energy of defects inside metals and heat dissipation. In Fig. 4, σ_{tr} denotes the critical martensitic transformation stress. It is defined as the intersection of the lines that are tangent to the initial elastic part and the upper plateau of the stress–strain curve.

The curve marked as "experimental" is plotted from real measurement data. It is noticed that the actual temperature rise takes place near the strain in correspondence to the determined transformation stress. Then the temperature continuously increases during

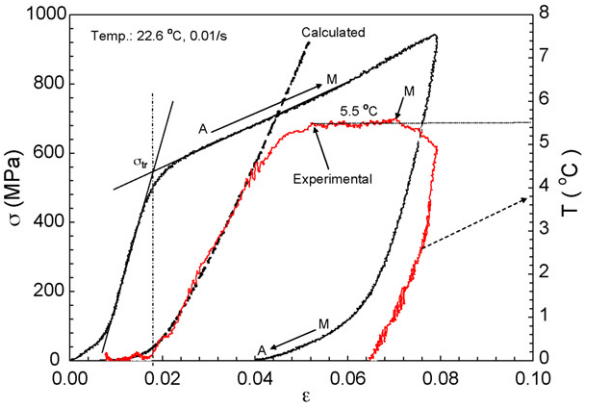

Fig. 4. Schematic illustration of atomic vibration or moves.

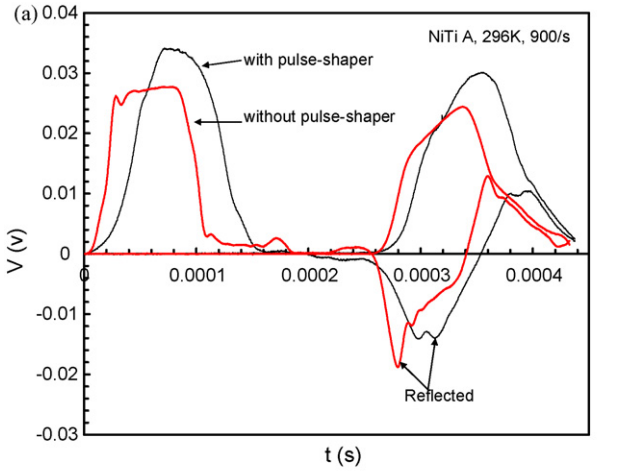

Fig. 5. Experimental results from Hopkinson bar tests: (a) strain pulse comparison; (b) stress and strain rate as functions of strain with and without a pulse shaper.

the transition from austenite to martensite until it arrives to a constant value somewhere in the middle of the transition procedure. The temperature begins to drop after passing point *M*, which indicates an end of martensitic transformation. During this loading test, the maximum temperature rise is about 5.5 °C. By observing Fig. 4, the following inspirations are obtained through this test: (i) the temperature rise is resulted from the transformation from austenitic phase to martensitic phase; (ii) the temperature rise can be roughly estimated by Eq. (2). Knowing that temperature has a strong effect on phase transition in NiTi SMAs, one can expect that this increased temperature actually enhanced the recovery ability from martensite to austenite. A higher strain rate can result in a higher temperature rise, and therefore the rate effect on behavior of SMAs is actually a combination of the effects from both strain rate and temperature change. Note that a finite temperature increase generally does not change the characteristic of stress-induced martensitic transformation. Therefore, we do not consider such temperature change due to applied strain rate in Section 3.3.

3.3. Measurement of the velocity for stress-induced martensitic transformation

In this experiment a batch of NiTi-A specimens are annealed at 473 K for 30 min to make sure that the specimens are in austenitic phase at room temperature of 296 K. These specimens are then put for uniaxial compressive loading tests at constant strain rates. Quasi-static compressive tests with strain rates of 10^{-3}–10^{-1}/s are performed on the electromechanical testing machine. The corresponding strain is measured by a strain extensometer directly attached to the sample. The dynamic tests with higher strain rates up to 4000/s are performed using an enhanced Hopkinson bar facility with 12.7 mm diameter bars. A mini Hopkinson bar facility with 5 mm diameter bars is used for strain rates higher than 4000/s. It is been noticed that the loading and unloading strain rates (reflected strain pulse) usually do not show constant value during the Hopkinson bar tests. A pulse shaper is used to achieve a constant strain rate during both loading and unloading. Here a special soft copper tube is placed on the impact end of the incident bar to modify impact pulses. Fig. 5 shows the results from the Hopkinson bar tests, with and without using a pulse shaper. By comparing the results, one notices that an almost constant strain rate can be achieved with such pulse shaper. Therefore, the pulse shaper is always used to get the stress–strain curves of NiTi-A for high strain rate tests.

The measured results for strain rates up to 2500/s are shown in Fig. 6a, and the corresponding results for the higher strain rates are shown in Fig. 6b. According to the plotted stress–strain curves, the stress-induced transformation from austenite to martensite can barely exist when the strain rate is around 7000/s. Although martensitic transformation still takes place at a strain rate between 2500 and 7000/s, the samples cannot completely recover their original shape. About 1.5% of residual strain is found. It implies that once the applied strain rate is around 7000/s, the displacive diffusionless shear-like mechanism of deformation changes to a dislocation-based slip plasticity. Samples of NiTi-A essentially deform as ordinary austenite metals, such that the measured stress–strain curves almost do not show any pseudoelastic behaviors. Finally, to confirm the behaviors between the strain rate of 7500 and 13,000/s, we did a separate test with 9000/s and the results are plotted in Fig. 6c. It is apparent that the pseudoelasticity has been gone at this strain rate.

The imposed deforming velocities of the samples in the tests can be obtained through Eq. (3), where the original height of the specimens, l_0, is equal to 5 mm. The martensitic transformation stresses, σ_{tr}, are determined as described in Fig. 4. Finally the deforming velocities and transformation stresses are plotted in Fig. 7 as functions of applied strain rate. The deforming velocity corresponding to a strain rate of 7000/s is 35 m/s. The transformation stress is approaching a constant value of 700 MPa as the applied strain rate is getting higher than 0.1/s.

$$\omega = l_0 \frac{d\varepsilon}{dt} \tag{3}$$

As it has been discussed earlier, once applied strain rate exceeds a critical value, the displacive diffusionless shear-like mechanism of deformation is replaced by dislocation-based slip plasticity. This means that the critical strain rate is corresponding to a deforming velocity that the velocity for stress-induced martensitic transition

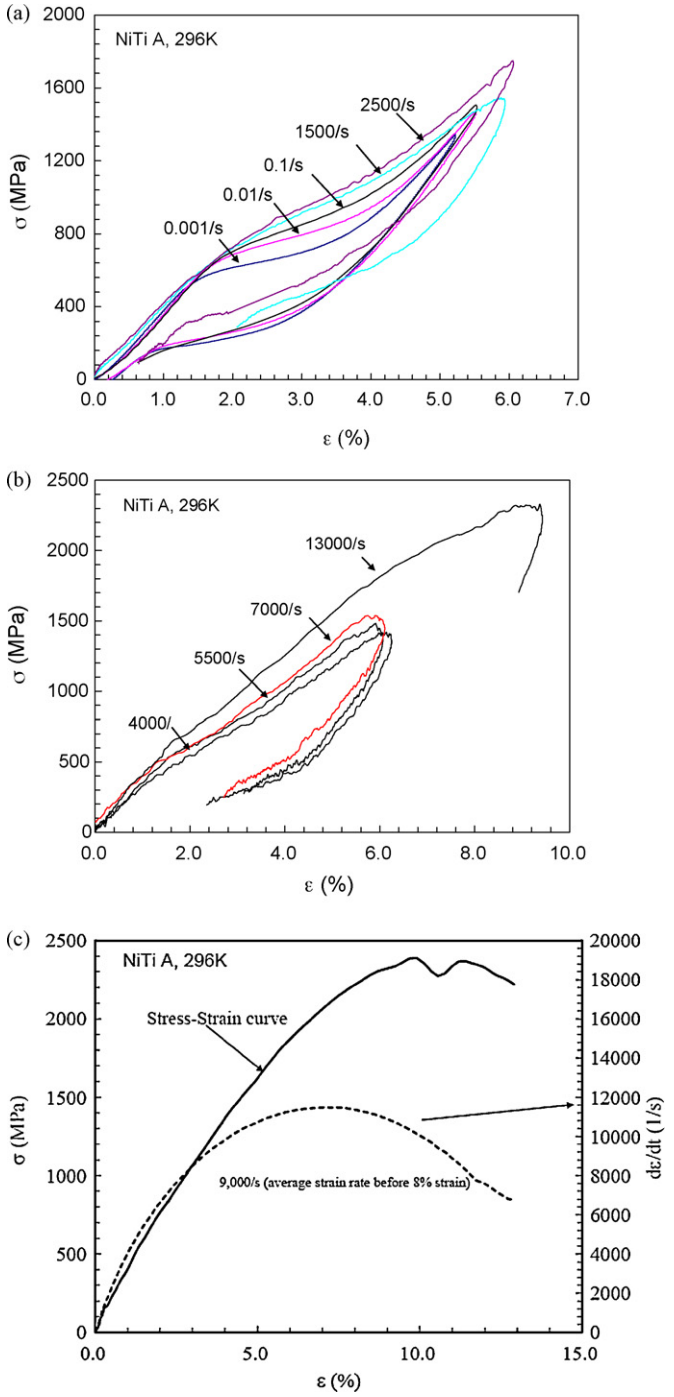

Fig. 6. Stress–strain curves for pseudoelastic tests: (a) results for strain rates from 0.001 to 2500/s; (b) results for strain rates from 4000 to 13,000/s; (c) results for strain rates of 9000/s.

cannot exceed. In another words, the highest observed deforming velocity (roughly 35 m/s here) that allows pseudoelastic behaviors is the corresponding velocity for a stress-induced martensitic transition in NiTi-A, or at least its measured upper bound. Therefore, through the testing results listed in this subsection, we have presented a feasible way to evaluate the real limit for stress-induced martensitic transition. It should be noticed that the calculated velocities are rough estimates, and may serve better as qualitative references. One needs to obtain more data around the critical strain rate to improve the accuracy of the evaluation. It is also noticed that the obtained velocity by the presented approach is much lower than

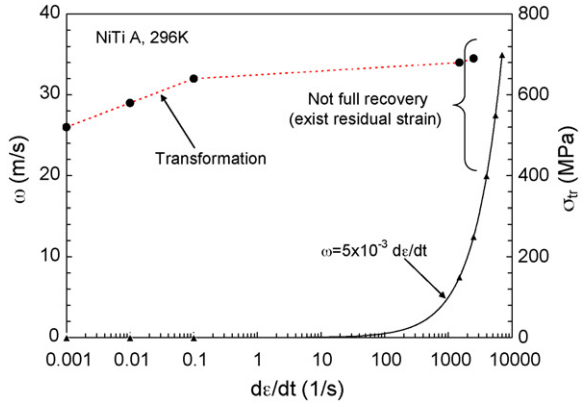

Fig. 7. Deforming velocity and transformation stress as functions of applied strain rate during the stress-induced martensitic transformation.

the theoretical estimate of 3000 m/s. There may be multiple reasons for that. One of the reasons is that the obstacles within the material can slow down the displacive transformation and consequently result in a lower velocity.

3.4. Measurement of recovery velocity for thermally driven reverse transformation

A fundamental question in applications of shape memory effect is, what is the recovery velocity for detwinned martensitic phase to transform back to austenite and how is the velocity affected by different amounts of temperature increase? In this subsection, we are going to experimentally find the recovery velocity and discuss the corresponding temperature effect. Specimens from NiTi-B are used for the measurement of recovery velocity. As mentioned before their crystal lattice structures maintain as martensitic twins at room temperature of 296 K. These samples are then tensioned at room temperature using an Instron servohydraulic testing machine at a constant rate of 0.001/s. During the testing a thermocouple and a strain extensometer are always attached to the sample to monitor the temperature and deformation. After being tensioned there will be certain residual strain left in each sample. These strained samples are then put in a loading free condition and heated by resistance heaters. As the applied temperature gets higher the strained samples will gradually recover to their original shape. It is been observed that the maximum recovery strain upon heating is 3%, as shown in Fig. 8. Therefore the following discussions are limited to samples with residual strains less than 3% only.

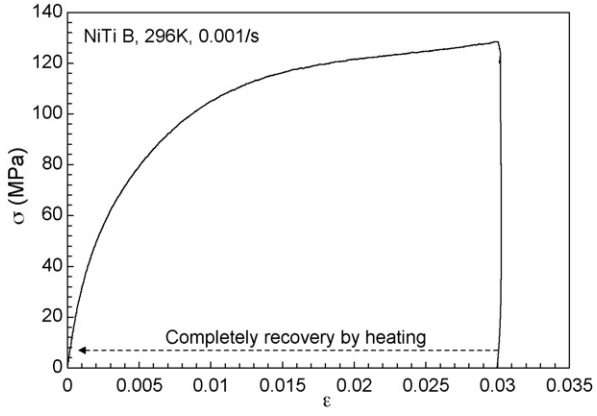

Fig. 8. Stress–strain relation for the recovery test at a temperature of 296 K and 0.001/s strain rate.

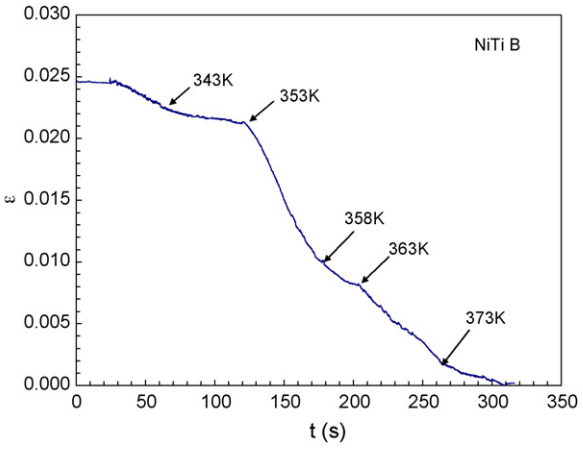

Fig. 9. Strain recovery history with linearly increased temperature.

Fig. 9 shows a strain recovery history of NiTi-B, which is experiencing a multi-point temperature increases from the room temperature. A strained specimen is heated from 296 to 343 K, and then to 353, 358, 363, and 373 K, as marked in Fig. 9. Note that it takes a few seconds to heat the sample from one temperature to another. Usually it takes about 10 s to heat a sample from room temperature to 400 K. It is noticed that the residual strain decreases as a function of time and is completely gone shortly after the temperature arrives at 37 3K. There is a dramatic drop of strain after the temperature is increased to 353 K. To further explore the recovery procedure, another strain recovery tests are performed under controlled temperatures above A_f of NiTi-B. Fig. 10 shows the strain recovery history curves at different constant temperatures. It is observed that the samples are recovering their original dimensions at constant rates. One can get a higher recovery strain rate with elevated temperature. The recovery strain rate is approaching to a constant value of limit once the temperature is higher than 363 K. Fig. 11 shows the total time spent for strain recoveries of 2.5% with different applied temperatures. Given the effective longitudinal dimension of the tested samples as 25 mm, one can obtain the recovery velocity for reverse transformation as a function of the applied temperature, as plotted in Fig. 12. Note that the limit for the recovery velocity is about 0.014 mm/s, which is measured at temperature of 373 K. By comparison, the velocity of thermally driven detwinned martensite to austenite transition is much less than the velocity of stress-induced martensitic transformation.

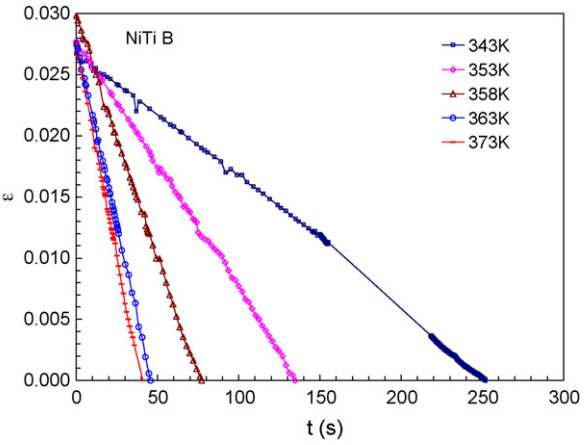

Fig. 10. Strain recovery history under fixed temperatures.

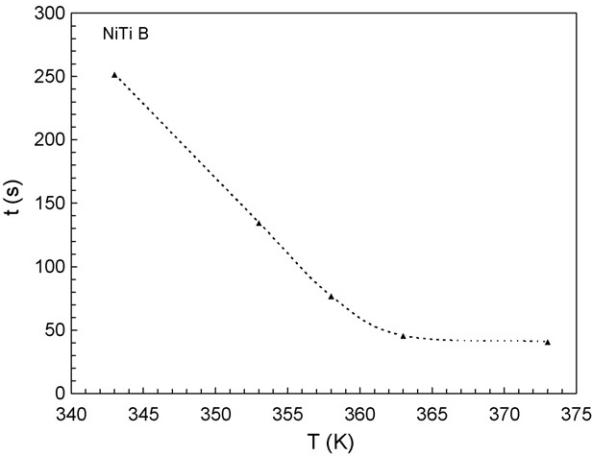

Fig. 11. The time spent for strain recovery of 2.5% as a function of applied temperatures.

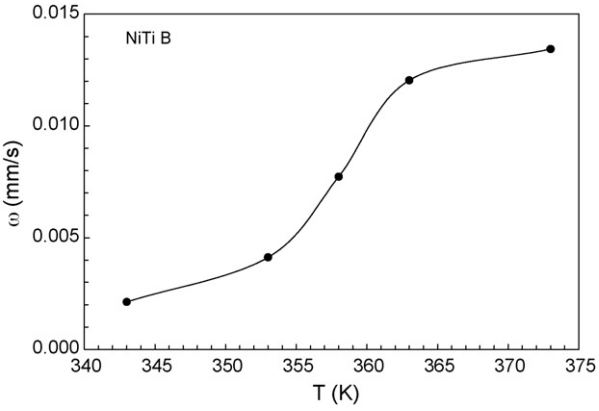

Fig. 12. The recovery velocity as a function of applied temperatures.

4. Concluding remarks

In this paper, both of the thermally driven and stress-induced phase transformations in NiTi SMAs are investigated. As key factors for the efficiency, applicability and reliability of SMAs devices, the velocity for stress-induced martensitic transformation and the recovery velocity for detwinned martensite to transform back to austenite are considered. First the limiting velocity for phase transition is theoretically estimated to be of the order of 10^3/s based on atomic vibration knowledge. Then the real velocities are experimentally evaluated through a series of pseudoelasticity loading tests and thermally driven strain recovery tests, respectively.

During the pseudoelasticity dynamic loading test, a copper tube pulse shaper is employed in the Hopkinson bar facility to help achieve a constant stain rate. It is been noticed that the stress-induced martensitic transformation is accompanied by temperature rise during the adiabatic process at a constant strain rate of 0.01/s, the maximum increased temperature is about 5.5 °C. Since temperature rise can inversely enhance the recovery ability from martensite to austenite, and higher strain rate will result in a higher temperature rise, the strain rate effect on behaviors of SMAs is essentially considered as a combined effect of both strain rate and temperature change. It is noticed during the uniaxial loading test that the pseudoelastic behavior tends to disappear as the imposed strain rate increases to a certain level. Based on the proposed theory that pseudoelasticity will not exist once the deforming velocity is higher than the velocity of stress-induced martensitic transition, the real velocity limit for a stress-induced martensitic transition in

NiTi-A can be measured as the highest observed deforming velocity that allows pseudoelastic behaviors.

As for the measuring of recovery velocity for NiTi-B, samples with martensitic twins are uniaxially tensioned at room temperature, such that the martensitic phase is detwinned and the samples are left with residual strains. It is been observed that the maximum recovery strain for NiTi-B is 3%. The tests are performed with multi-point temperature increases and fixed temperatures. During the multi-point temperature increases, the recovery strain rate is nonlinear with respect to time, and the maximum recovery strain rate occurs around the temperature of 353 K. But once the heating temperature is fixed, one gets constant recovery strain rate. Finally, the observed upper bound for recovery velocity during the thermally driven reverse transformation from detwinned martensite to austenite is about 0.014 mm/s.

Acknowledgements

The work is supported by National Natural Science Fund of China (10872169) and by State Key Laboratory of Explosion Science and Technology, Beijing Institute of Technology (KFJJ08-11). Authors also thank the support from Science and Technology Fund of Shaanxi, China (2007K06-11) and Beijing Municipal Education Commission project (10842002).

References

[1] K. Otsuka, X. Ren, Intermetallics 7 (1999) 511–528.
[2] J.A. Shaw, S. Kyriakdes, J. Mech. Phys. Solids 43 (8) (1995) 1243–1281.
[3] K. Otsuka, C.M. Wayman, Shape Memory Materials, Cambridge Unversity Press, 1998, pp. 27–48.
[4] S. Nemat-Nasser, W.G. Guo, Mech. Mater. 38 (2006) 463–474.
[5] S. Nemat-Nasser, J.Y. Choi, W.G. Guo, et al., J. Eng. Mater. Technol. 127 (2005) 83–89.
[6] S Nemat-Nasser, J.Y. Choi, W.G. Guo, et al., Mech. Mater. 37 (2–3) (2005) 287–298.
[7] S. Zhuiykov, Sens. Actuators A 141 (2008) 89–96.
[8] Y. Bellouard, Mater. Sci. Eng. A 481–482 (2008) 582–589.
[9] T. Namazu, A. Hashizume, S. Inoue, Sens. Actuators A 139 (2007) 178–186.
[10] Y. Dong, Z. Boming, L. Jun, Mater. Sci. Eng. A 485 (2008) 243–250.
[11] H. Tobushi, Y. Shimeno, et al., Mech. Mater. 30 (1998) 141–150.
[12] Y. Liu, Z. Xie, J.V. Humbeeck, Mater. Sci. Eng. A A273–275 (1999) 673–678.
[13] M.A. Meyers, Dynamic Behavior of Materials, John Wiley & Sons, Inc., New York, USA, 1994, pp. 5–50.
[14] S. Nemat-Nasser, Y. Su, W.G. Guo, et al., J. Mech. Phys. Solids 53 (2005) 2320–2346.